

REDOX STORAGE SYSTEMS FOR SOLAR APPLICATIONS

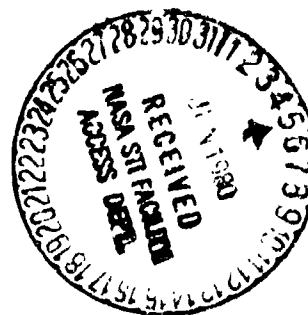
(NASA-TM-81464) REDOX STORAGE SYSTEMS FOR
SOLAR APPLICATIONS (NASA) 28 P
HC A03/MF A01 CSCL 10A

N80-23777

Unclas
G3/44 20320

Norman H. Hagedorn and Lawrence H. Thayer
National Aeronautics and Space Administration
Lewis Research Center

Work performed for
U.S. DEPARTMENT OF ENERGY
Energy Technology
Energy Storage Systems Division



Prepared for
Power Sources Conference
Brighton, England, September 15-18, 1980

NOTICE

This report was prepared to document work sponsored by the United States Government. Neither the United States nor its agent, the United States Department of Energy, nor any Federal employees, nor any of their contractors, subcontractors or their employees, makes any warranty, express or implied, or assumes any legal liability or responsibility for the accuracy, completeness, or usefulness of any information, apparatus, product or process disclosed, or represents that its use would not infringe privately owned rights.

REDOX STORAGE SYSTEMS FOR SOLAR APPLICATIONS

Norman H. Hagedorn and Lawrence H. Thaller
National Aeronautics and Space Administration
Lewis Research Center
Cleveland, Ohio 44135

Prepared for
U.S. DEPARTMENT OF ENERGY
Energy Technology
Energy Storage Systems Division
Washington, D.C. 20545
Under Interagency Agreement EF-77-A-31-1002

Power Sources Conference
Brighton, England, September 15-18, 1980

ERRATA

DOE/NASA/1002-80/5
NASA Technical Memorandum 81464

REDOX STORAGE SYSTEMS FOR SOLAR APPLICATIONS

Norman H. Hagedorn and Lawrence H. Thaller
September 1980

Page 13: Equation (7) should be

$$\frac{2kA\theta}{V} = 9.594 \times 10^{-4} \left(\frac{D_{Fe} \theta U' UC}{iT} \right) \quad (7)$$

where $C = 1$ mole per liter.

Figure 5: Six lateral lines should be added to the center boxes to complete the circuit diagram (see attached figure).

Figure 9: The equation should be

$$\frac{C}{C_o} = \frac{1}{2} \left\{ \exp \left[-6.14 \times 10^{-4} \left(\frac{D_{Fe}}{iT} \right) \theta \right] + 1 \right\}$$

Figure 9: The heading for the third column in the table should be i .

REDOX STORAGE SYSTEMS FOR SOLAR APPLICATIONS

Norman H. Hagedorn, Lawrence H. Thaller

Lewis Research Center
National Aeronautics and Space Administration
Cleveland, Ohio 44135, U.S.A.

ABSTRACT

E-383

The world-wide development of solar photovoltaic and wind turbine systems to meet a range of terrestrial electrical energy requirements has underscored the need for inexpensive and reliable electrical energy storage. The NASA Redox Energy Storage System based on soluble aqueous iron and chromium chloride redox couples has displayed many system-related features which for the most part are unique to this storage system. The needed technology advances in the two elements (electrodes and membranes) that are key to its technological feasibility have been achieved and system development has begun. The design, construction, and test of a one kilowatt system integrated with a solar photovoltaic array is underway to provide early demonstration of the attractive system-related features of the NASA Redox Storage system, its versatility and its compatibility with a terrestrial solar photovoltaic electric power system.

INTRODUCTION

For years man has been working on concepts and devices that would allow him to harness even a small fraction of the energy that is associated with the sun. Much has been achieved from a scientific and engineering point of view but wide-spread commercial applications have

been very limited because of the ready availability of inexpensive, reliable electrical energy that was able to meet expanding needs. Within the last decade there has been an abrupt turnabout in the cost and availability of energy in the "developed" nations as well as an increasing awareness on the part of "undeveloped" nations of their lack of many of the things that are taken for granted in these other societies. This has stimulated, among other solar technologies, wide-spread development efforts directed towards solar photovoltaic and wind turbines as sources of electrical energy. The associated requirement for inexpensive long lived, reliable electrical energy storage will pace the broad deployment and commercial growth of non-grid connected or "stand-alone" systems.

A typical important stand-alone system application is a remote village with no power lines available to be extended to the village or a situation in which it is more cost effective to install a solar powered generator (solar photovoltaic or wind turbine) in conjunction with the appropriate amount of energy storage to supply the overall load requirements during periods of darkness, storms, windless days, etc. The NASA Lewis Research Center has, in conjunction with the Department of Energy and the Agency for International Development, designed, installed, and maintains several small, stand-alone remote village solar photovoltaic power system application demonstrations. One of these is located in Schuchuli, Arizona, USA and the other in Tangaye, Upper Volta, Africa (Rosenblum, et. al. 1979). These demonstrations have successfully shown the feasibility of such village power

supplies. In both cases these systems operate nominally at 120 volts DC to reduce power distribution losses as well as to take advantage of the widespread commercial availability of 120 volt DC universal motors for water pumping, household appliances, etc. In these demonstrations lead-acid batteries have served as the energy storage device.

The potential short-comings of lead-acid batteries for these types of applications are related to cost, reliability, maintenance, charge control, cell imbalance and life. Among the growing number of advanced battery concepts being developed as possible replacements for lead-acid batteries is the NASA Redox energy storage system.

NASA Redox Energy Storage System

The NASA Redox concept was first described in 1974 (Thaller, 1974). Briefly, it is based on the use of two fully-soluble redox couples and a highly selective ion exchange membrane which almost completely prevents any cross-mixing of reactant cations and yet allows free passage of the non-reactant anions. Storage tanks for reactant solutions (one tank per reactant) and circulating pumps make up the remaining components of the system. Figure 1 schematically illustrates the basic system. Stacks of cells hydraulically connected in parallel and electrically connected in series using a bipolar plate arrangement was conceived. This concept required the development of ion exchange membranes with selectivities that would reduce the cross diffusion rates of reactant ions by several orders of magnitude over the then current state-of-the-art for ion

exchange membrane materials, and the identification of two suitable fully soluble redox couples. About four years of active development work brought forth the required enabling technologies in these areas. Further, a number of system-related features were devised to enhance the overall operational performance of this rapidly advancing technology. These features are discussed in depth elsewhere (Thaller 1979). A Redox system that incorporates these features is called a full function system and is shown schematically in figure 2.

Figure 3 shows an expanded view of the single cell (the repeating unit) and a complete full function stack. The ion exchange membrane forms the heart of each individual cell. This material is a fabric-supported ion exchange membrane typically 0.035 cm thick formed by the polymerization of vinylbenzylchloride and dimethylaminoethyl-methacrylate. Other pertinent room temperature properties of this membrane appear in Table 1, and further information on the development of cross-linked polyelectrolyte membranes for Redox applications can be found elsewhere (Alexander, et. al. 1979). On either side of the membrane is the porous, flow-through electrode that is compressed between the bipolar plate material and the membrane. Currently, carbon felt (catalyzed in the case of the chromium electrode) is used with thin carbon bipolar plates (approx. 0.9 mm). The cell cavities are formed by the combination of the gasket and flow plate. These items are both die-cut from polyethylene sheet material. The flow plate contains the inlet and exit ports that are carefully designed to

give the required ionic resistance between the flow manifolds and the active portion of the cell. Dielectric washers are required in the manifold region of the electronically conductive bipolar plates and the ionically conductive membranes to reduce shunt current losses to a minimum. An in-depth treatment of this subject has been published (Prokopius, 1976).

Aside from the system-related features already mentioned, the illustration of figure 3 shows what appears to be extra terminal plates at one end of the stack (labeled "trim cells").

These trim cells are another system-related feature which is of particular importance for solar applications. These cells, placed at the end of the basic stack, with switching, can be added to the basic stack when a higher system voltage is required and removed when not required. Intermediate voltage levels can also be selected by appropriate connections to the Redox stack. Figure 4 illustrates a few of the many possible variations that are available. Illustrated here is a single stack. The overall stack is thus seen to consist of a recombination cell, an open circuit voltage cell, a 14-cell substack followed by a 40-cell substack followed by two 2-cell substacks. As drawn, all 60-cells are connected hydraulically in parallel. The stack would have an unregulated output of about 12 volts and a regulated output of about 50 ± 2 volts or 38 ± 2 volts depending on the take-off point selected.

When the charging options are considered, the permutations and

combinations of possible electrical arrangements expand considerably. It should be pointed out, for example, that this stack could be charged across the 12 volt terminals and simultaneously discharged across the regulated 50 volt terminals. There are many other charging and discharging possibilities. Such a versatile electrochemical storage system should meet many storage needs more effectively than other candidate systems.

Possible Solar Array/Redox System Configurations

The possible ways of arranging individual solar cells in series strings and series/parallel panels is rather large. One such multikilowatt arrangement used by the Lewis Research Center, shown in figure 5 as a block diagram, consists of the parallel arrangement of high voltage (e.g., 120 volts DC) strings of cells. The addition of a Redox system to this type of solar array arrangement can be done in at least four different ways, as depicted in figure 6. Here again, system details are deleted. The operation of each of these arrangements are as follows:

a. The Redox system is floated across the main array supply bus. In this mode the rate of charge and the degree of load sharing is controlled by the setting of the trim cell selector (automatically controlled by suitable logic and switching devices). It should be noted here, as well as in the following examples, that no switching from "charge" to "discharge" is required.

b. & c. The Redox stack is placed between the solar panels and the

load. In the first case (b) trim cell switching is provided on the load side of the stack and is used to maintain proper voltage regulation. Charge control is provided by switching the solar p

In the second case (c) there is trim switching on the solar array as well as the load side of the stack. This arrangement allows an extension of the charging capabilities of the solar array to lower voltage levels:

d. Separate charging stack and discharging stacks are used. This arrangement, of course, is based on the fact that the solutions that are charged are returned to the storage tanks from which the discharge stack would draw its fluids. In this arrangement it is quite obvious that a different voltage level can be used in the charging stack than that is used in the discharging stack.

One kW Solar Array/Redox System

The design of the system is based on case b where a single connection is made on the charge side of the Redox stack and multiple attachments are available on the discharge side of the stack (figure 7). In brief, there are four separate substacks connected hydraulically in parallel and electrically in series. The schematic includes instrumentation for all parameters to be measured. The net output of the system is designed at 1.0 kW at about 30 ma/cm² steady state operation with the capability of peaking to 2.0 kW at about 65 to 70 ma/cm² operation. Further details appear in Table 2. A capacity of about 11 to 12 kWhr was selected as one that although not particularly

representative of a solar stand-alone application (40 hours of storage is more representative), was felt to be great enough to allow the evaluation of overall system performance and storage/solar array interactions. The considerations that resulted in this particular selection of number of cells, cell size, flow rate, charging conditions, control logic, etc., stem in part from:

- a. the present status of a steadily advancing set of technologies (i.e., membranes, pumps, electrodes, certain electronic components);
- b. the system characteristics which in part are inherent to flow batteries in general or Redox systems in particular (i.e., shunt current, pumping losses, flow requirements, voltage vs. depth-of-discharge characteristics);
- c. the arbitrary selection of certain system specifications (i.e., watt hour capacity, voltage level, regulation requirement, depth-of-discharge span).

System Design Methodology

A. System Volume

One liter of a one molar solution contains one Faraday (26.8 ampere hour) of electrical charge for a one electron reaction. This is the starting point for determining the system volume requirements to satisfy a given storage capacity, but two corrections must be made to adjust this value. One results from the fact that it is very difficult to make full use of all the oxidizable or reducible ions

that are present in the solution because their concentration approaches zero at the ends of charge and discharge and thus mass transport becomes a problem. The second stems from the fact that there is a gradual loss of active species across the not quite perfect ion exchange membrane.

The selection of the depth of discharge span is a result of flow rate, pumping losses, and reactant requirement considerations that can only be alluded to here. Over the course of a charge or discharge of a redox couple there is a wide variation in the concentration of the oxidized and reduced species. These changing concentrations can be related to changing flow requirements that are needed to supply the ionic reactions that produce the current within these cells. The flow requirements for systems that have a Redox solution as one of their reactants actually double each time the concentration of the reactant species is halved (1.0M .5M .25M .125M .0625M etc.). The stoichiometric flow rate (and thus the required pumping power) approaches infinity as the reactant concentration approaches zero. Further, the Nernstian correction factor as applied to the open circuit voltage of 1.075 volts/cell at 50% state of charge is also changing very rapidly at the far ends of the span. Table 3 simply lists the stoichiometric flow requirements of a 1000 cm² cell operating at either 50 ma/cm² or 100 ma/cm² at different depths of charge (states of charge) during charge and discharge when 1.0 Molar solutions are used. Included in this table are the approximate open circuit voltage (OCV) values at various states of charge. These stoichiometric flow rate values vary linearly with cell area,

current density and reactant concentrations. Actual cell charge and discharge performance at various flow rates and states of charge must be obtained to accurately assess all the effects that are present in these flow-through electrodes.

Figure 8 illustrates the type of data that are required to help evaluate the relative performance of various types of electrodes and cell structures as well as to quantitatively show the relative importance of mass transport, Nernstian and internal resistance effects. At high flow rates (low concentration changes from inlet to outlet) there should be minimal mass transport contributions to the shape of this set of curves. The spacing between the curves is thus related to the internal resistance of the cell. At lower flow rates the bulk flow concentration change across the cell is such that the Nernstian correction to the cells "average" reversible potential is dependent on the current density and flow rate. Also in this region the ability to diffuse to and from the slowly moving reactant stream and the electrode becomes more of a problem, even though the electrode is porous. A condition is finally reached where the flow rate (number of reactant species ions entering the cell per unit of time) just balances the impressed current density (reaction rate). By definition, this is called the stoichiometric flow rate and at this point the cell performance drops abruptly. Good cells are thus ones that, although they are subject to the Nernstian droop at low flow rates, have a minimum of concentration polarization. Figure 8 is typical of what is felt to be reasonably good performance from the

standpoint of being able to operate close to the stoichiometric flow rate.

If a constant speed pump is to be used, a compromise must be made in the selection of flow rate. The net result of these and other considerations led to the selection of a span between 80% and 20% depth of discharge for this experimental system, with the expectation that future systems will be cycled between 90% and 10% depth of discharge.

Another consideration affecting tankage volume is related to the rate of loss of reactant species due to diffusion through the membranes. This leads to a permanent loss of usable capacity of the system and indeed is the only cause of permanent capacity loss. For the membranes used in the system this cross diffusion rate, as measured in static membrane tests, is initially about 12 micrograms of iron per hour per square centimeter, when a one molar iron solution is allowed to diffuse across the membrane into a solution that initially contains no iron. Translated to the system level, the actual rate of capacity loss would be an exponential function of 1) the membrane area across which the cross diffusion takes place (which in turn is related to the current density for which the system is designed, 2) the initial volume (capacity of the system), and 3) the cross diffusion parameter of the membrane. The equation takes the form,

$$\frac{C}{C_0} = 1/2 \left(e^{\frac{-2kA_0}{V}} + 1 \right) \quad (3)$$

Where

C = concentration of reactant, mols/liter
 C_0 = initial concentration of reactant, mols/liter
 A = total cell (membrane) active area, cm^2
 V = total volume of one reactant, liters
 k = diffusion coefficient, $\text{liters}/(\text{cm}^2)(\text{hr})$
 θ = total time of system operation, hours.

Evaluation of the exponent involves the following considerations: The membrane area (A) is determined by the design power output of the system, the design current density and an average single cell voltage. Reactant volume (V) is related to the actual watt-hours storage, the average cell voltage, the utilization (depth of discharge span), the solution concentration and an added over-capacity incorporated at the beginning of life to compensate for the gradual capacity loss that results from membrane cross mixing.

$$A = \frac{P}{i v_{av}} \quad (4)$$

$$V = \frac{PT}{nFv_{av}CUU'} \quad (5)$$

Where

P = design power, watts
 T = duration at design power, hours
 v_{av} = overall average cell voltage during discharge, volts
 n = equivalents per mole
 F = ampere hours per equivalent
 C = concentration, moles per liter
 U = fractional utilization of reactants due to depth of discharge span

U' = fractional utilization of reactants due to excess used at beginning of life

i = current density milliamps/cm²

The diffusion coefficient (k) in Equation 3 is related to the experimentally measured parameter D_{Fe} by the following equation (for iron):

$$k_{Fe} = \frac{D_{Fe} \left(\frac{\mu\text{gm}}{\text{hr} \cdot \text{cm}^2 \cdot \text{mol/l}} \right) \times \left(\frac{10^{-6} \text{gm}}{\mu\text{gm}} \right)}{55.85 \text{ gm Fe/mol}} \quad (6)$$

$$= 1.79 \times 10^{-8} D_{Fe}, \text{ l/cm}^2\text{-hr}$$

Therefore,

$$\frac{2kAO}{V} = 9.594 \times 10^{-4} \left(\frac{D_{Fe} \theta U' U}{iT} \right) \quad (7)$$

After substituting the above for the exponent, equation 3 can be used to calculate the remaining iron concentration after θ hours of operation.

This θ would correspond to the lapsed time following the initial startup of the system if the pumps were to run at all times.

Figure 9 gives an example of the C/Co ratio as a function of the time a system is subject to the maximum cross diffusion conditions.

A summary example of the corrections made to the "ideal" for a system requiring calculated reactant volume is as follows:

(For 100 units of end-of-life energy storage) $100 \times 1.25 \times 1.33 =$
167 units of original capacity are installed to compensate for these

two factors (80% depth of discharge span and 25% membrane cross diffusion loss).

The time to 25% loss for other combinations of cross diffusion rate (D_{Fe}), storage duration (T), and current density (membrane area for diffusion) are linearly related to the results plotted here.

B. Stack Size

Figure 10 illustrates the information required to be able to size the stack part of the overall Redox system. Although other information is required it forms the core or basis for the first approximation.

In this case the lines are generated from an assumed effective area resistivity of $6.1 \Omega\text{-cm}^2$. Several arbitrary selections of voltage regulation limits and overall system net output are also needed.

Figure 10 is simply a series of current voltage plots over the range of selected depth of discharge boundaries at the design flow rate of reactants using the cell components (membrane type, electrolyte type, and cell flow configuration) to be used in the final stack. For the case in point, the single cell characteristics are such that at 50% depth of discharge the average single cell voltage will be 0.88 volts at a current density of 32 ma/cm^2 . The hardware on hand is 320 cm^2 active area (0.33 ft^2) and the nominal system voltage level was to be 120 volts DC $\pm 5\%$. These factors led to a gross output of $10 \text{ amps} \times 120 \text{ volts} = 1.20 \text{ kW} \pm 5\%$. An 80% depth of discharge line would intercept the 32 ma/cm^2 line at an average cell voltage of 0.81 volts; thus a conservative estimate of the total number of cells required would be $(120)(1.05)/0.81 = 156 \text{ cells}$. (The smallest total would be

$(120)(.95)/0.81 = 141$ cells. As the state of charge is increased, or the current density decreased, trim cell packages are shed to keep within the voltage regulation limits. The number six was selected for the number of single cells to be included in each of ten trim packages. The number of trim packages is closely related to the effective resistance of the individual cells (Figure 10). The goal during 1980 is to produce membranes such that the present design value of 28 milliwatts/cm² at 50% depth of discharge at 0.9 volts per cell will be extended to 54 milliwatts/cm². Our current best cell value is 41.5 milliwatts/cm².

From the gross power output must be subtracted the shunt power losses, the pumping power requirements and any instrumentation requirements. The shunt power losses (as predicted by Prokopius, 1976) increase with about the third power of the number of cells in the stack. Shunt losses were minimized by designing the inlet and outlet ports of the cells such that high ionic resistance paths between the active area of the cell and the inlet and outlet manifolds were present, yet acceptable pressure drops for the flow of the reactant fluids existed. Typical flow rate vs. pressure drop data obtained from a single cell appears in figure 11. Shunt losses were further reduced by splitting the hydraulics into four parallel paths, each feeding a thirty-nine cell substack. At a maximum charging voltage of between 1.25 and 1.30 volts per cell, the expected shunt loss per substack is about 20 watts. Inter-stack losses are estimated at about 45 watts, total. The currently available magnetically coupled centrifugal pumps have an

overall efficiency of about 15 to 20% for one that will deliver 5.0 gallons per minute at a 10 psia head. These efficiencies are viewed to be too low for a practical Redox system, but do serve adequately for this experimental test of the concept. The power requirements of these pumps are expected to be 100 watts each.

C. Instrumentation and Controls

One important reason for conducting the system test is to explore the operating characteristics of a complete system that is capable of being placed in field service and cycled in some random manner. The system electrical diagram (figure 7) shows the ability to record the individual cell voltages on a data logger at preselected time intervals, plus the more usual bookkeeping type of data of watt-hours and ampere-hours, in and out, for the various parasitic loads, etc.

For the switching in and out of trim cell packages, a series of meter relays with progressively wider tolerance set points will be used in this test, with the expectation that as the control measurements become more firmly fixed, an appropriate microprocessor can be designed.

CONCLUSIONS

At this writing all membranes, electrodes bipolar plates, end blocks, end plates, pumps, tanks, fittings, test fixtures and hardware are on hand and stack assembly has begun. It is the current plan to build and test each substack on a special purpose test stand prior to its

acceptance into the 1.0 kW system. Initial checkout testing will begin in March of 1980. Field testing is scheduled to follow successful completion of the initial test program which will be carried out at the Solar Photovoltaic Test Facility located at the Lewis Research Center.

The results of this test program will clearly document the advantages of Redox storage systems.

Table 1

Properties of Membrane Formulations Used
In 1.0 kW Redox System

Designation - CD1L-A5-27.5NP

Area Resistivity ($\Omega\text{-cm}^2$)

.1N HCl	- 4.6
1.0N HCl	- 3.6
1.0M FeCl_3 , 2.0N HCl	- 6.23

Thickness - .035 cm

Water Content - 36%

Ion Exchange Capacity - milli. equiv./dry gram

Strong	- 2.01
Weak	- 2.35
Total	- 4.36

Selectivity - 12 micrograms of iron/hr/ $\text{cm}^2/\text{M}/\ell$

Table 2

Redox System Design Parameters

Gross Power	1260 watts
Nominal Net Power	1000 watts
Voltage	120 \pm 5%, VDC
Number of Stacks	4
Number of Cells/Stack	39
Trim Packages	10 packages, 6 cells each
Depth of Discharge Range (Utilization)	80% - 20% (0.60)
Reactant Volume (Each)	700 ℓ (186 U.S. gallons)
Reactant Energy Density	14.5 Wh/ ℓ
Cell Active Area	320 cm^2
Nominal Current Density	30 ma/ cm^2
Reactants	1M/ ℓ FeCl_3 , 2N HCl 1M/ ℓ CrCl_2 , 2N HCl
Reactant Flow Rates (Nominal)	100-150 $\text{cm}^3/\text{min.}$ - cell
Parasitic Losses	Pumps - 200 watt Shunt Currents - 125 watt
Number of Rebalance Cells	5
Number of Charge-Indicator Cells	1

Table 3

Stoichiometric Flow Requirements of
1000 cm² Cells Operating at 50 ma/cm²
and 100 ma/cm² Employing 1 Molar Solutions

Depth of Discharge (%)	State of Charge (%)	Approx. OCV	During Charge			During Discharge		
			50 ma/cm ²	100 ma/cm ²	50 ma/cm ²	100 ma/cm ²	50 ma/cm ²	100 ma/cm ²
0	100	-	∞	∞	∞	∞	31.1 cm ³ /min	62.2 cm ³ /min
10	90	1.195	310.9 cm ³ /min	621.8 cm ³ /min	34.6	69.1	34.6	69.1
25	75	1.130	124.4	248.8	41.5	82.9	41.5	82.9
50	50	1.075	62.2	124.4	62.2	124.4	62.2	124.4
75	25	1.020	41.5	82.9	124.4	248.8	124.4	248.8
90	10	0.955	34.6	69.1	310.9	621.8	310.9	621.8
100	0	-	31.1	62.2	∞	∞	∞	∞

$$\text{Stoichiometric Flow Rate (cm}^3\text{/min)} = \frac{\text{Current Density} \times \text{Area}}{1.608 \frac{\text{Amp. Min.}}{\text{cm}^3} \times \text{Fractional State of Charge}}$$

References

1. Rosenblum, L., Bifano, W.J., Hein, G.F., and Ratajczak, A.F., (1979), "Photovoltaic Power Systems for Rural Areas of Developing Countries," NASA TM-79097.
2. Thaller, L.H., (1974), "Electrically Rechargeable Redox Flow Cells," Proceedings Ninth IECEC p. 924.
3. Thaller, L.H., (1979), "Redox Flow Cell Energy Storage Systems," NASA TM-79143, DOE/NASA/1002-79/3.
4. Alexander, S.S., Hodgdon, R.B., and Waite, W.A., (1979), "Anion Permselective Membranes," NASA CR-159599, DOE/NASA/0001-79/1.
5. Prokopius, P.R., (1976), "Model for Calculating Electrolytic Shunt Path Losses in Large Electrochemical Energy Conversion Systems," NASA TMX-3359.

ORIGINAL PAGE IS
OF POOR QUALITY

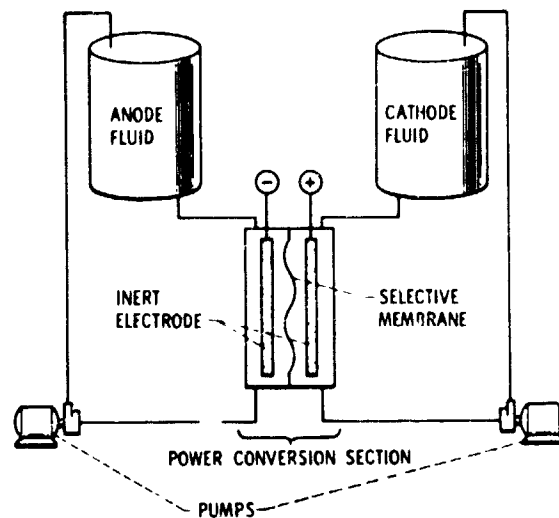


Figure 1. - The basic redox flow cell schematic.

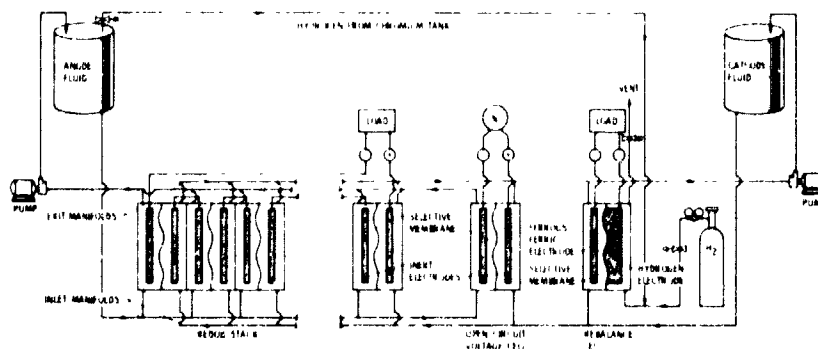


Figure 2. - Schematic diagram of a full function redox energy storage system using the fully soluble iron and chromium redox couples.

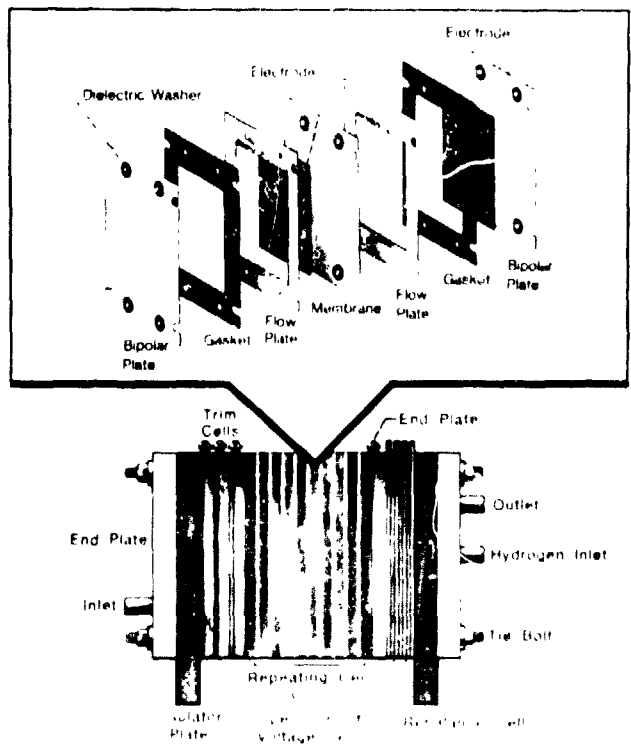


Figure 3 - Exploded view of a single cell assembly with an expanded view of the single cell components.

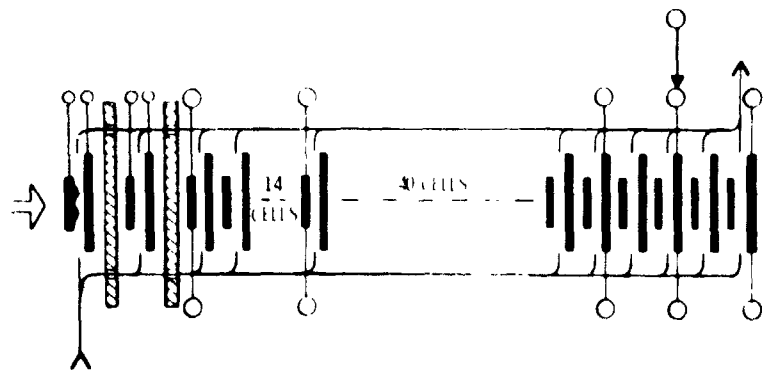


Figure 4 - Diagrammatic representation of a possible redox stack configuration.

ORIGINAL PAGE IS
OF POOR QUALITY

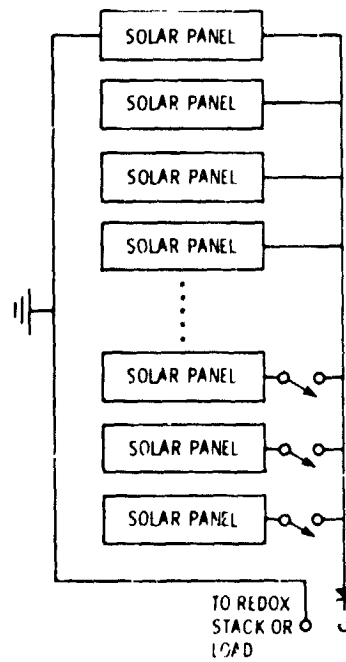


Figure 5. - Schematic diagram of the voltage control technique used for adjustment of photovoltaic output voltage.

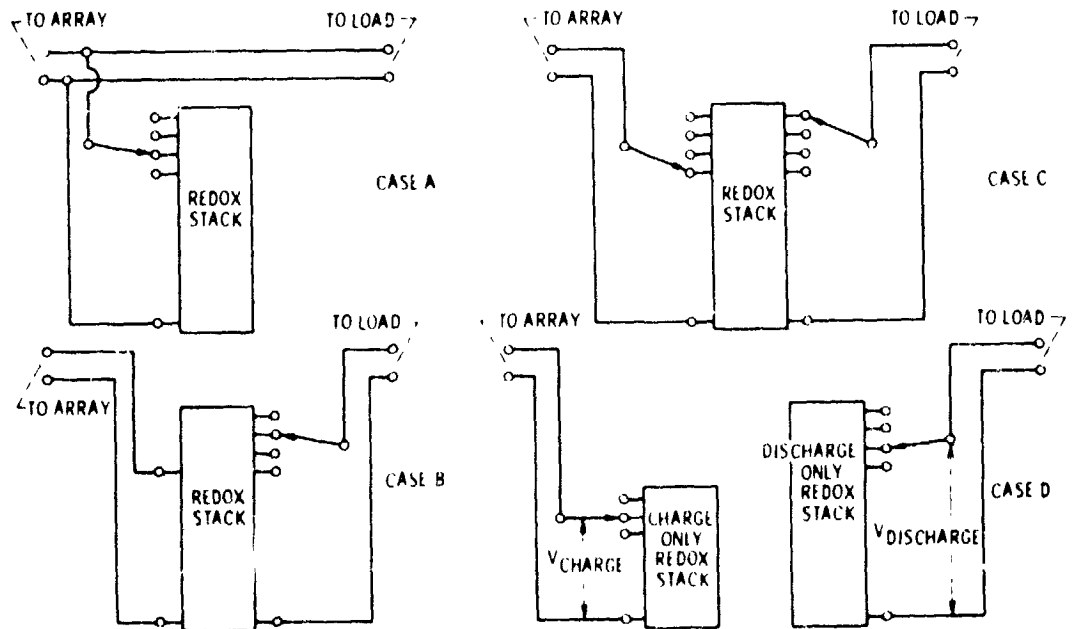


Figure 6. Schematic diagram of possible ways to interconnect the photovoltaic energy source to the Redox Energy Storage subsystem. Case A. Redox stack floated on main solar array bus. Case B. Fixed input voltage and trimmed output voltage. Case C. Trimmed input voltage and trimmed output voltage. Case D. Separate charge and discharge stacks.

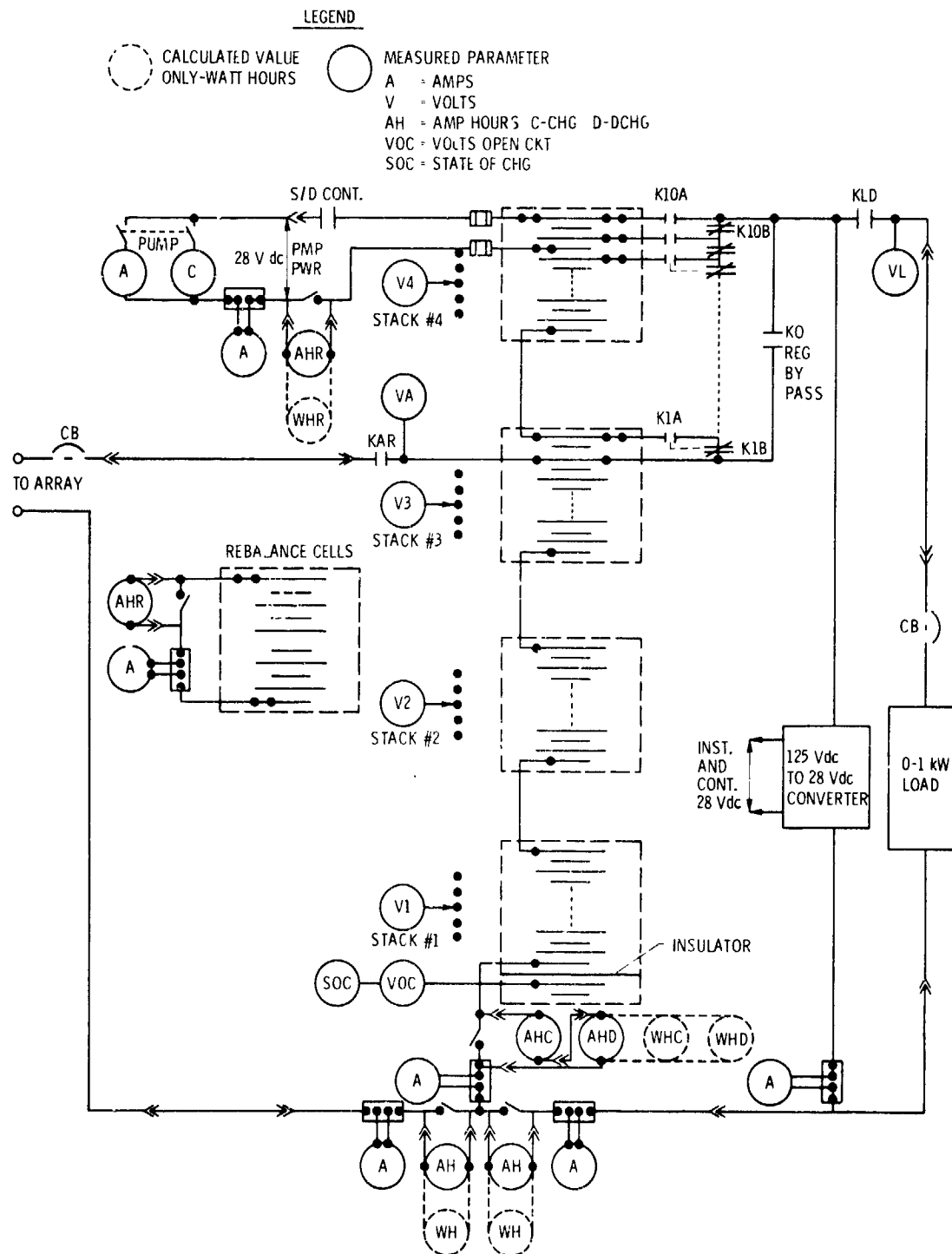


Figure 7. - Electrical diagram of the 1.0 kilowatt system showing instrumentation and data acquisition points.

ORIGINAL PAGE IS
OF POOR QUALITY

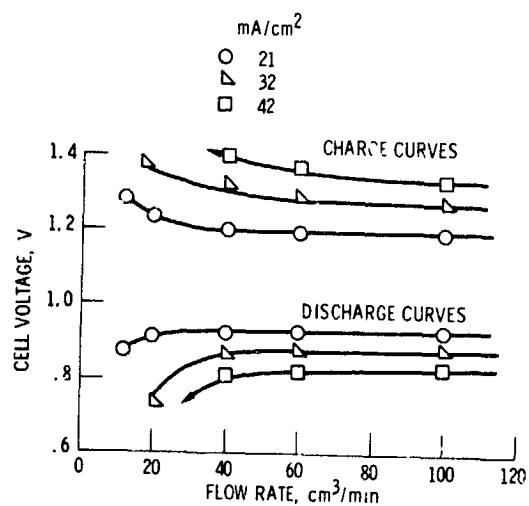


Figure 8. - Performance map of a typical 320 cm² cell at 50 percent depth of discharge.

$$\frac{C}{C_0} = \frac{1}{2} \left\{ \exp \left[-6.14 \times 10^{-4} \left(\frac{D_{Fe}}{iT} \right) \theta \right] + 1 \right\}$$

$u = 0.8 \quad u' = 0.8$

D_{Fe}	T	$\frac{1}{iT}$
10	50	50
5	50	25
5	25	50

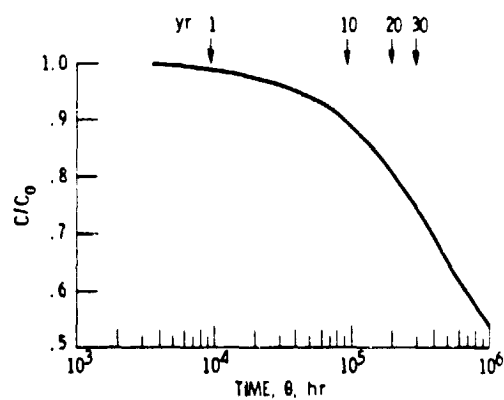


Figure 9. - Predicted capacity decay with time for several combinations of storage times, membrane diffusion characteristics and average current densities.

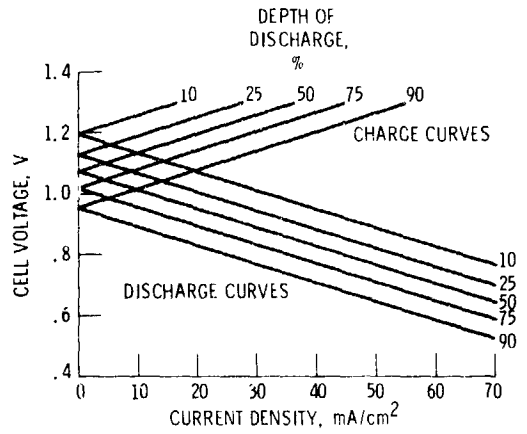


Figure 10. - Current-voltage characteristics of a cell with an assumed effective internal resistance of $6.1 \Omega\text{-cm}^2$ and reversible behavior. The various open circuit voltage values were obtained using the 1.075 volt values at 50 percent depth of discharge and applying the Nernstian corrections.

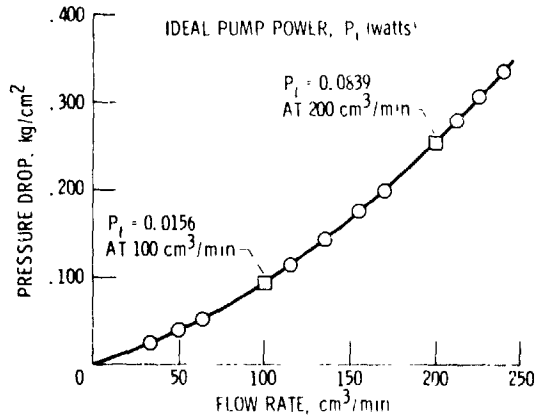


Figure 11. - Pressure drop data as a function flow rate for a typical 320 cm^2 half cell using water as the working fluid. This information permits the calculation of ideal pumping power (P_t) requirement for actual Redox hardware.

1 Report No NASA TM-81464	2 Government Accession No	3 Recipient's Catalog No	
4 Title and Subtitle REDOX STORAGE SYSTEMS FOR SOLAR APPLICATIONS		5 Report Date	
		6 Performing Organization Code	
7 Author(s) Norman H. Hagedorn and Lawrence H. Thaller		8 Performing Organization Report No E-383	
		10 Work Unit No	
9 Performing Organization Name and Address National Aeronautics and Space Administration Lewis Research Center Cleveland, Ohio 44135		11 Contract or Grant No	
		13 Type of Report and Period Covered Technical Memorandum	
12 Sponsoring Agency Name and Address U.S. Department of Energy Energy Storage Systems Division Washington, D.C. 20545		14 Sponsoring Agency Code Report No. DOE NASA /1002-80/5	
15 Supplementary Notes Prepared under Interagency Agreement EC-77-A-31-1002. Prepared for Power Sources Conference, Brighton, England, September 15-18, 1980.			
16 Abstract <p>The world-wide development of solar photovoltaic and wind turbine systems to meet a range of terrestrial electrical energy requirements has underscored the need for inexpensive and reliable electrical energy storage. The NASA Redox Energy Storage System based on soluble aqueous iron and chromium chloride redox couples has displayed many system-related features which for the most part are unique to this storage system. The needed technology advances in the two elements (electrodes and membranes) that are key to its technological feasibility have been achieved and system development has begun. The design, construction, and test of a 1 kilowatt system integrated with a solar photovoltaic array is underway to provide early demonstration of the attractive system-related features of the NASA Redox Storage system, it's versatility and its compatibility with a terrestrial solar photovoltaic electric power system.</p>			
17 Key Words (Suggested by Author(s)) Energy storage Redox Batteries		18 Distribution Statement Unclassified - unlimited STAR Category 44 DOE Category UC-94c	
19 Security Classif. (of this report) Unclassified	20 Security Classif (of this page) Unclassified	21 No of Pages	22 Price*